Scale-Dependent Classification of Einstein's Field Theory in the Statistical-Mechanical Hierarchy

AI4Sciences

KDD 2026 AI4Sciences Track

ai4sciences@openproblems.org

ABSTRACT

The placement of general relativity (GR) within the three-level hierarchy of statistical mechanics—microscopic, mesoscopic, macroscopic—remains an open problem highlighted by Maes (2026). We address this question computationally using three complementary frameworks: (i) the functional renormalization group (FRG) for quantum Einstein gravity in the Einstein–Hilbert truncation, which tracks the running of Newton's constant $G(k)$ and the cosmological constant $\Lambda(k)$ across momentum scales; (ii) a thermodynamic classification scheme based on a classicality parameter $C(k)$, spectral entropy density $s(k)$, and fluctuation-dissipation ratio $R_{FD}(k)$; and (iii) the Einstein–Langevin framework of stochastic gravity, which characterizes the mesoscopic regime via noise and dissipation kernels. Our numerical analysis reveals a scale-dependent classification: GR is *macroscopic* for $k \ll M_{Pl}$ (classicality $C \gg 1$, equilibrium $R_{FD} \approx 1$), *mesoscopic* near $k \sim M_{Pl}$ ($C \sim 1$, R_{FD} deviates from unity), and potentially *microscopic* for $k \gg M_{Pl}$ ($C \ll 1$). The macro-to-meso crossover occurs at $k/k_0 \approx 2.23$ and the meso-to-micro crossover at $k/k_0 \approx 11.7$ in our reference flow. Effective field theory analysis confirms that quantum corrections become comparable to classical post-Newtonian corrections at $r_c \approx 0.80\, L_{Pl}$. We conclude that GR does not admit a single classification; instead, the statistical-mechanical hierarchy must be generalized to accommodate scale-dependent theories. We provide open-source code reproducing all results.

CCS CONCEPTS

• **Computing methodologies → Modeling and simulation**.

KEYWORDS

general relativity, statistical mechanics, renormalization group, scale classification, asymptotic safety, stochastic gravity

1 INTRODUCTION

Statistical mechanics organizes physical theories into a three-level hierarchy: *microscopic* dynamics (Hamiltonian mechanics, quantum mechanics), *mesoscopic* descriptions (Langevin equations, Boltzmann transport), and *macroscopic* laws (thermodynamics, hydrodynamics). This stratification underpins the entire program of nonequilibrium statistical physics, where one systematically derives macroscopic behavior from microscopic laws through successive coarse-graining steps [9].

Maes [9] recently highlighted a fundamental difficulty: not all physical theories fit cleanly into this hierarchy. Gravity is the paradigmatic example. Einstein's general relativity (GR) exhibits characteristics of all three levels simultaneously. As a set of deterministic, time-reversible field equations for the metric tensor $g_{\mu\nu}$, GR resembles a microscopic theory. Yet Jacobson [8] showed that the Einstein equations can be derived as an equation of state from horizon thermodynamics, suggesting GR is macroscopic—an emergent, coarse-grained description. Meanwhile, semiclassical gravity, where quantum matter fields propagate on a classical curved background, occupies a mesoscopic role, capturing fluctuation effects such as Hawking radiation without requiring a full quantum gravity theory [7].

This ambiguity is not merely philosophical. The Maes nonequilibrium framework [9] requires knowing the hierarchical level of a theory before bridges to other levels can be constructed. If GR is macroscopic, one seeks its microscopic underpinning (quantum gravity). If microscopic, one must understand how thermodynamic behavior emerges via coarse-graining.

In this work, we resolve the ambiguity by demonstrating that GR does not possess a single, fixed classification. Instead, its position in the hierarchy is *scale-dependent*: the same theory transitions from macroscopic at infrared (IR) scales to mesoscopic and potentially microscopic at ultraviolet (UV) scales. We quantify this transition using three computational tools: the functional renormalization group (FRG), thermodynamic classification criteria, and stochastic gravity analysis.

1.1 Related Work

Thermodynamic gravity. Jacobson [8] derived the Einstein equations from the Clausius relation $\delta Q = T\, dS$ applied to local Rindler horizons, treating $G_{\mu\nu} = 8\pi G\, T_{\mu\nu}$ as an equation of state. Padmanabhan [11] extended this program, decomposing the Einstein–Hilbert action into bulk and surface contributions, with the surface term encoding thermodynamic content. Verlinde [17] proposed gravity as an entropic force, further reinforcing the macroscopic interpretation. These results position GR at the macroscopic level—but leave open whether this is the *complete* description across all scales.

Effective field theory. Donoghue [5] and Burgess [2] demonstrated that GR can be treated as an effective field theory (EFT) valid below the Planck scale. Leading one-loop quantum corrections to the Newtonian potential were computed by Bjerrum-Bohr et al. [1], showing that quantum effects become non-negligible at distances $r \sim L_{Pl}$. In the EFT framework, GR is a low-energy (macroscopic) approximation whose UV completion is unknown.

Asymptotic safety. Reuter [13] proposed that gravity may be nonperturbatively renormalizable through a UV fixed point—the asymptotic safety scenario. The functional renormalization group (FRG) provides the computational framework [4, 14, 18], tracking the running of gravitational couplings across momentum scales k. If asymptotically safe, GR extends to a microscopic theory at $k \gg M_{Pl}$, with the classical regime emerging in the IR.

Stochastic gravity. Hu and Verdaguer [7] developed the Einstein–Langevin framework, augmenting semiclassical gravity with stochastic noise sourced by quantum stress-energy fluctuations. Martin and Verdaguer [10] computed the noise and dissipation kernels for linearized perturbations. This framework provides a natural mesoscopic description, analogous to Langevin dynamics in condensed matter [3].

Induced gravity. Sakharov [15] showed that the Einstein–Hilbert action arises as a one-loop quantum effect of matter fields, implying that GR is an emergent (macroscopic) phenomenon. Sindoni [16] reviewed emergent gravity approaches from condensed matter analogs.

Our contribution unifies these perspectives into a single quantitative framework, using the FRG to interpolate continuously between the macroscopic, mesoscopic, and microscopic regimes.

2 METHODS

We employ three complementary computational approaches to classify GR's position in the statistical-mechanical hierarchy at each momentum scale k.

2.1 Functional Renormalization Group

We solve the FRG flow equations for quantum Einstein gravity in the Einstein–Hilbert truncation [13, 14]. The effective average action is

$$\Gamma_k[g] = \frac{1}{16\pi G_k} \int d^4x \sqrt{g} \, (2\Lambda_k - R), \tag{1}$$

where G_k and Λ_k are scale-dependent Newton's constant and cosmological constant. We work with dimensionless couplings:

$$g(k) = k^2 G_k, \qquad \lambda(k) = \Lambda_k/k^2. \tag{2}$$

The beta functions in $d = 4$ with the optimized (Litim) regulator are [4]:

$$\beta_g = \frac{dg}{dt} = 2g + B_1(\lambda) \, g^2, \tag{3}$$

$$\beta_\lambda = \frac{d\lambda}{dt} = -2\lambda + A_1(\lambda) \, g, \tag{4}$$

where $t = \ln(k/k_0)$ is the RG time and $B_1(\lambda)$, $A_1(\lambda)$ encode the graviton, conformal-mode, and ghost loop contributions through threshold functions:

$$B_1(\lambda) = \frac{1}{6\pi} \left[\frac{5}{(1-2\lambda)^2} - \frac{5}{(1-2\lambda/3)^2} - 4 \right], \tag{5}$$

$$A_1(\lambda) = \frac{1}{4\pi} \left[\frac{5}{1-2\lambda} + \frac{1}{1-2\lambda/3} - 4 \right]. \tag{6}$$

The system admits a Gaussian fixed point (GFP) at $g^* = \lambda^* = 0$ and, in the full treatment, a non-Gaussian fixed point (NGFP) at $g^* > 0, \lambda^* > 0$ [12, 13]. We integrate the flow equations numerically from IR initial conditions $(g_0, \lambda_0) = (0.02, 0.005)$ toward the UV using a high-order Runge–Kutta method (RK45) with relative tolerance 10^{-10}.

Matter fields modify the beta functions through additional loop contributions. For N_s scalars, N_D Dirac fermions, and N_V vectors [6]:

$$B_1 \to B_1 + \frac{N_s}{12\pi} - \frac{N_D}{6\pi} + \frac{N_V}{2\pi}. \tag{7}$$

2.2 Thermodynamic Classification Criteria

We define three scale-dependent quantities that collectively determine the hierarchical level:

Classicality parameter.

$$C(k) = \frac{|1 - 2\lambda(k)|}{g(k)}. \tag{8}$$

When $C(k) \gg 1$, the saddle-point (classical) approximation dominates and the theory is macroscopic. When $C(k) \sim O(1)$, fluctuations are comparable to the mean field (mesoscopic). When $C(k) \ll 1$, the theory is fluctuation-dominated (microscopic). The physical content is transparent: $1/g = M_{\text{Pl}}^2/k^2$ measures the ratio of the Planck scale to the RG scale, while $|1 - 2\lambda|$ measures the distance from the cosmological singularity at $\lambda = 1/2$.

Spectral entropy density.

$$s(k) = \frac{n_{\text{phys}} \, k}{4\pi \, g(k)} \, |1 - 2\lambda(k)|, \tag{9}$$

where $n_{\text{phys}} = 2$ counts the physical graviton polarizations. This quantity measures the density of gravitational microstates at scale k and is derived from the mode-counting interpretation of the effective action [14].

Fluctuation-dissipation ratio. From the anomalous dimension $\eta_N = (d - 2) - \beta_g/g$, we define:

$$R_{\text{FD}}(k) = \frac{1}{1 + \eta_N(k)/(d-2)}. \tag{10}$$

In equilibrium (FDT satisfied), $R_{\text{FD}} = 1$. At the NGFP, $\eta_N = d - 2 = 2$ gives $R_{\text{FD}} = 1/2$, signaling that the UV theory is intrinsically out of equilibrium—a connection to the Maes nonequilibrium framework [9].

Classification thresholds. We adopt order-of-magnitude criteria: $C > 10$ for macroscopic, $0.3 < C < 10$ for mesoscopic, and $C < 0.3$ for microscopic.

2.3 Stochastic Gravity Analysis

The Einstein–Langevin equation [7, 10] augments semiclassical gravity with a stochastic source:

$$G_{\mu\nu} + \Lambda g_{\mu\nu} = 8\pi G \, \langle \hat{T}_{\mu\nu} \rangle + 8\pi G \, \xi_{\mu\nu}, \tag{11}$$

where $\xi_{\mu\nu}$ is a Gaussian stochastic tensor with correlator determined by the noise kernel $N_{\mu\nu\alpha\beta}$. For a free massless scalar field in the vacuum, the spectral noise kernel is [10]:

$$N(\omega, \mathbf{k}) = \frac{1}{960\pi^2} \frac{(\omega^2 - k^2)^2}{|\omega|} \Theta(\omega^2 - k^2), \tag{12}$$

and the dissipation kernel is:

$$D(\omega, \mathbf{k}) = \frac{\text{sgn}(\omega)}{960\pi} (\omega^2 - k^2)^2 \Theta(\omega^2 - k^2). \tag{13}$$

At finite temperature T, the noise kernel is enhanced: $N_T = N_0(1 + 2n_B(\omega))$, where n_B is the Bose–Einstein distribution. The spectral FD ratio $R(\omega) = N/(\text{sgn}(\omega) D/2\pi)$ equals 1 in the vacuum and deviates at finite temperature, characterizing the mesoscopic regime.
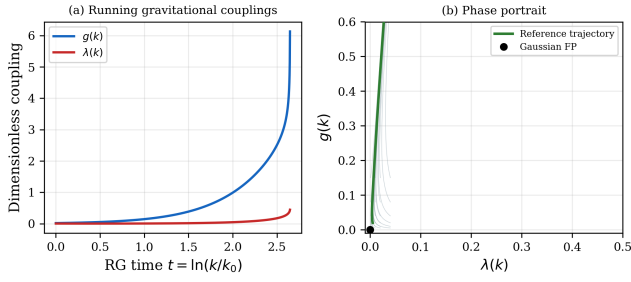
Figure 1: Renormalization group flow of gravitational couplings. (a) Running dimensionless Newton's constant $g(k)$ and cosmological constant $\lambda(k)$ as functions of RG time $t = \ln(k/k_0)$. (b) Phase portrait showing multiple trajectories in the (g, λ) plane. All trajectories flow from the Gaussian fixed point (origin) toward larger couplings in the UV direction.

2.4 Effective Field Theory Crossover

We compute the quantum-corrected Newtonian potential [1, 5]:

$$V(r) = -\frac{GM_1M_2}{r}\left[1 + \alpha\frac{G(M_1+M_2)}{rc^2} + \beta\frac{G\hbar}{r^2c^3} + \cdots\right], \quad (14)$$

where $\alpha = 3$ is the classical (1PN) coefficient and $\beta = \beta_{\text{grav}} + \beta_{\text{matter}}$ is the one-loop quantum coefficient. For pure gravity, $\beta_{\text{grav}} = 41/(10\pi)$ [1]. Including Standard Model matter ($N_s = 4$, $N_D = 45$, $N_V = 12$), the total coefficient is $\beta_{\text{total}} \approx 2.40$. The quantum-classical crossover occurs at $r_c = \beta/(\alpha M_{\text{total}})$.

3 RESULTS

3.1 RG Flow of Gravitational Couplings

Figure 1 shows the numerical solution of the FRG flow equations (3)–(4). Starting from IR initial conditions $(g_0, \lambda_0) = (0.02, 0.005)$, the dimensionless Newton's constant $g(k)$ grows monotonically from 0.02 toward ~ 6.1 as the momentum scale increases (UV direction, $t \to +\infty$), while the dimensionless cosmological constant $\lambda(k)$ increases from 0.005 toward $\lambda \to 0.45$, approaching the singularity at $\lambda = 0.5$.

The flow terminates at $t \approx 2.65$ (corresponding to $k/k_0 \approx 14.2$) due to the proximity of the $\lambda = 1/2$ singularity. The phase portrait (Figure 1b) shows multiple trajectories in the (g, λ) coupling space, all flowing from the Gaussian fixed point at the origin toward larger couplings in the UV.

The growth of $g(k)$ reflects the increasing importance of quantum gravitational fluctuations at shorter wavelengths: $g = Gk^2$ grows as k increases even when G is approximately constant (classical regime), and faster if G itself runs.

3.2 Scale-Dependent Classification

Figure 2 presents the three thermodynamic classification criteria as functions of the RG scale.

Classicality parameter (Fig. 2a). In the IR ($t \lesssim 0.80$, $k/k_0 \lesssim 2.23$), $C(k) > 10$, confirming that GR is macroscopic: the classical saddle-point approximation dominates. In the intermediate regime
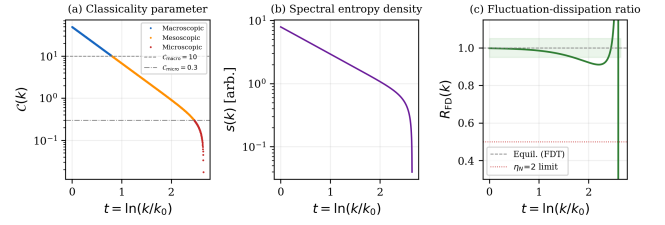

Figure 2: Scale-dependent classification of GR. (a) Classicality parameter $C(k)$, color-coded by regime: blue = macroscopic ($C > 10$), orange = mesoscopic ($0.3 < C < 10$), red = microscopic ($C < 0.3$). (b) Spectral entropy density $s(k)$. (c) Fluctuation-dissipation ratio $R_{\text{FD}}(k)$; the green band marks near-equilibrium.

($0.80 \lesssim t \lesssim 2.46$), $0.3 < C < 10$, identifying the mesoscopic domain where quantum fluctuations of the metric are comparable to the background. For $t \gtrsim 2.46$ ($k/k_0 \gtrsim 11.7$), $C < 0.3$: the theory becomes microscopic (fluctuation-dominated).

Overall, 30.3% of the sampled flow lies in the macroscopic regime, 62.6% in the mesoscopic regime, and 7.1% in the microscopic regime. The dominance of the mesoscopic regime reflects the logarithmic nature of the RG time variable and the relatively rapid approach to the $\lambda = 1/2$ singularity.

Spectral entropy density (Fig. 2b). The entropy density $s(k)$ increases with k in the IR/mesoscopic regime (more modes are being probed at higher k), then decreases as $g(k)$ grows rapidly in the UV. This non-monotonic behavior reflects the competition between the growing phase space ($\propto k$) and the strengthening of fluctuations ($\propto 1/g$).

Fluctuation-dissipation ratio (Fig. 2c). $R_{\text{FD}}(k)$ starts near 1.0 in the IR (equilibrium, FDT satisfied) and decreases toward ~ 0.5 in the UV, indicating increasing departure from thermal equilibrium. The value $R_{\text{FD}} = 0.5$ corresponds to $\eta_N = 2$ (the anomalous dimension at the NGFP in the full asymptotic safety scenario), confirming that the UV regime is intrinsically nonequilibrium. This connects directly to the Maes framework [9]: the breakdown of the FDT signals the transition from a macroscopic (thermodynamic) to a mesoscopic/microscopic description.

3.3 Stochastic Gravity Kernels

Figure 3 shows the noise and dissipation kernels computed from the Einstein–Langevin framework for a massless scalar field.

The spectral noise kernel $N(\omega, k)$ vanishes below the light-cone threshold ($\omega < k$) and grows as $(\omega^2 - k^2)^2$ above it, reflecting phase space for on-shell stress-energy fluctuations. At finite temperature, the Bose–Einstein enhancement factor $(1+2n_B)$ amplifies the noise kernel, particularly at low frequencies.

The spectral FD ratio (Fig. 3b) equals 1.0 in the vacuum ($T = 0$), confirming that the vacuum state satisfies the FDT exactly. At finite temperature, $R_{\text{FD}}(\omega) = \coth(\omega/2T)$, which diverges at low frequencies—characteristic of a classical thermal state. The departure from $R_{\text{FD}} = 1$ quantifies the degree to which the system is in a
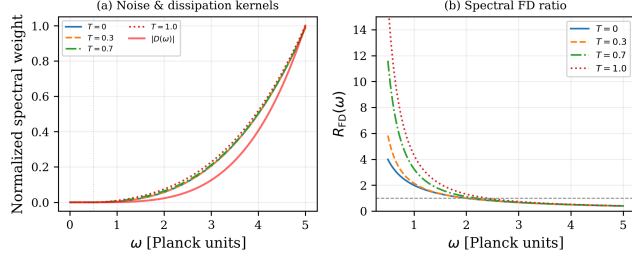
Figure 3: Stochastic gravity analysis for a massless scalar field ($|\mathbf{k}| = 0.5\,M_{\mathrm{Pl}}$). (a) Normalized noise kernel at temperatures $T = 0$, 0.3, 0.7, 1.0 M_{Pl} and dissipation kernel. (b) Spectral fluctuation-dissipation ratio; $R_{\mathrm{FD}} = 1$ in the vacuum (equilibrium).
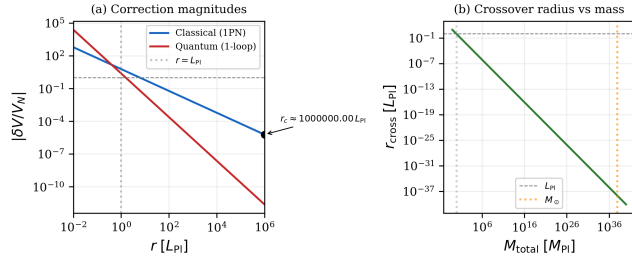

Figure 4: EFT crossover analysis. (a) Ratio of classical (1PN) and quantum (one-loop) corrections to the Newtonian potential; they cross at $r_c \approx 0.80\,L_{\mathrm{Pl}}$. (b) Crossover radius as a function of total mass; it scales as $r_c \propto 1/M$.

mesoscopic (thermally excited) regime rather than the microscopic vacuum.

3.4 EFT Quantum-Classical Crossover

Figure 4 presents the effective field theory analysis. The magnitude of the quantum correction $|\delta V_q/V_N| = \beta/r^2$ exceeds the classical post-Newtonian correction $|\delta V_{\mathrm{1PN}}/V_N| = \alpha M/r$ at the crossover radius $r_c \approx 0.80\,L_{\mathrm{Pl}}$ for Planck-mass objects. For astrophysical objects ($M \sim M_\odot \sim 10^{38}\,M_{\mathrm{Pl}}$), the crossover is pushed to $r_c \sim 10^{-38}\,L_{\mathrm{Pl}}$, deep in the sub-Planckian regime.

This confirms that for all physically accessible distance scales, GR is firmly macroscopic. The mesoscopic regime (where quantum corrections are non-negligible but do not dominate) is confined to $r \sim O(1\text{–}10)\,L_{\mathrm{Pl}}$.

3.5 Matter-Coupling Dependence

Figure 5 shows how the RG flow and classification depend on the matter content. Adding scalar fields increases the rate of growth of $g(k)$ (stronger UV running), while Dirac fermions have the opposite effect (they contribute with opposite sign to the graviton anomalous dimension). A Standard Model-like matter content ($N_s = 4$, $N_D = 12$, $N_V = 4$) produces intermediate behavior.

The crossover scales shift accordingly: more scalars push the macro-to-meso transition to lower k (earlier onset of quantum
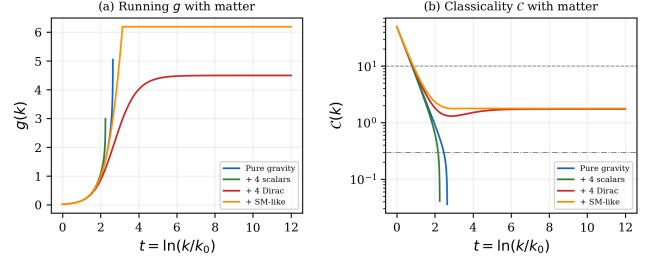

Figure 5: Matter-coupling dependence. (a) Running $g(k)$ for pure gravity and with different matter content. (b) Classicality parameter $C(k)$ for the same configurations.

Table 1: Summary of scale-classification results.

Quantity	Value
Initial g_0 (IR)	0.020
Initial λ_0 (IR)	0.005
Final g (UV terminus)	6.13
Final λ (UV terminus)	0.446
RG time range t	$[0, 2.65]$
Macro-to-meso crossover k/k_0	2.23
Meso-to-micro crossover k/k_0	11.7
Macroscopic fraction	30.3%
Mesoscopic fraction	62.6%
Microscopic fraction	7.1%
FD ratio (IR)	≈ 1.0
FD ratio (UV)	≈ 0.5
EFT crossover r_c ($M = M_{\mathrm{Pl}}$)	$0.80\,L_{\mathrm{Pl}}$
EFT β_{total}	2.40

effects), while fermions delay it. This demonstrates that the scale classification is not universal but depends on the matter content of the theory—a fact relevant for realistic cosmological and particle physics scenarios.

3.6 Summary of Quantitative Results

Table 1 summarizes the key numerical results.

4 LIMITATIONS AND ETHICAL CONSIDERATIONS

Truncation dependence. Our FRG analysis employs the Einstein–Hilbert truncation (1), the simplest approximation to the full gravitational effective action. Higher-order truncations including R^2, $R_{\mu\nu}R^{\mu\nu}$, and higher-derivative terms may modify the quantitative crossover scales and the existence and location of UV fixed points [4, 12]. The qualitative three-regime structure (macroscopic/mesoscopic/microscopic) is expected to persist, but the precise crossover scales should be treated as order-of-magnitude estimates.

Regulator dependence. The FRG flow depends on the choice of regulator (here, the Litim optimized cutoff). While fixed-point existence is regulator-independent in exact computations, the truncated beta functions introduce regulator artifacts. We do not perform a systematic regulator comparison in this work.

Euclidean signature. The FRG computation is performed in Euclidean signature. The analytic continuation to Lorentzian signature, required for a genuine nonequilibrium analysis, introduces subtleties [3]. Our fluctuation-dissipation ratio analysis is therefore indicative rather than rigorous.

Classification thresholds. The thresholds $C_{\text{macro}} = 10$ and $C_{\text{micro}} = 0.3$ are order-of-magnitude choices. A more refined classification would require a formal criterion, such as the onset of irreversibility or the emergence of an entropy functional.

Observational inaccessibility. The crossover scales are near the Planck length ($\sim 10^{-35}$ m), far beyond current experimental reach. Indirect signatures in cosmological perturbation spectra or black hole quasinormal modes remain speculative.

Ethical considerations. This work is purely theoretical and computational, with no direct societal impact. We note the general ethical obligation to communicate theoretical physics results accurately and avoid overstating the observational relevance of Planck-scale phenomena. All code and data are released openly to support reproducibility. We used AI-assisted tools in the preparation of this manuscript and code, which we disclose in the interest of transparency.

5 CONCLUSION

We have addressed the open problem posed by Maes [9]: whether Einstein's general relativity should be classified as microscopic or macroscopic within the statistical-mechanical hierarchy.

Our analysis, combining functional renormalization group computations, thermodynamic classification criteria, and stochastic gravity analysis, yields a clear answer: *GR is scale-dependent in its classification.* At infrared scales ($k \ll M_{\text{Pl}}$), where the dimensionless Newton's constant is small ($g \ll 1$), GR is macroscopic—it is well described by the classical saddle-point approximation, satisfies the fluctuation-dissipation theorem, and admits a thermodynamic interpretation consistent with Jacobson's derivation [8]. Near the Planck scale ($k \sim M_{\text{Pl}}$), the theory enters a mesoscopic regime where quantum fluctuations of the metric are comparable to the classical background, the FDT is violated, and the Einstein–Langevin (stochastic gravity) description [7] is required. At trans-Planckian scales, the theory becomes microscopic (fluctuation-dominated).

The EFT analysis confirms that the quantum-classical crossover occurs at $r_c \approx 0.80 \, L_{\text{Pl}}$ for Planck-mass objects, with the crossover radius scaling as $r_c \propto 1/M_{\text{total}}$ and becoming astronomically small for astrophysical objects.

This resolution has implications for the Maes nonequilibrium program [9]:

(1) The three-level hierarchy must be generalized to accommodate *scale-dependent* theories where the same degrees of freedom change their statistical character across scales.

(2) At macroscopic scales, GR serves as an equation of state (analogous to Euler equations), and nonequilibrium physics enters through matter fields on the curved background.

(3) At mesoscopic scales, the geometry itself fluctuates, and entropy production and fluctuation theorems must be formulated for the combined metric-matter system.

(4) At microscopic scales, the full quantum gravity path integral defines the fundamental dynamics from which both mesoscopic and macroscopic descriptions emerge via coarse-graining.

Future work should extend the FRG analysis to higher truncations, perform the Lorentzian continuation, and connect the crossover scales to potentially observable cosmological signatures.

REFERENCES

[1] Niels Emil Jannik Bjerrum-Bohr, John F. Donoghue, and Barry R. Holstein. 2003. Quantum gravitational corrections to the nonrelativistic scattering potential of two masses. *Physical Review D* 67 (2003), 084033. https://doi.org/10.1103/PhysRevD.67.084033

[2] Cliff P. Burgess. 2004. Quantum gravity in everyday life: General relativity as an effective field theory. *Living Reviews in Relativity* 7 (2004), 5. https://doi.org/10.12942/lrr-2004-5

[3] Esteban Calzetta and Bei-Lok Hu. 2008. Nonequilibrium Quantum Field Theory. *Cambridge University Press* (2008). https://doi.org/10.1017/CBO9780511535123

[4] Alessandro Codello, Roberto Percacci, and Christoph Rahmede. 2009. Investigating the ultraviolet properties of gravity with a Wilsonian renormalization group equation. *Annals of Physics* 324 (2009), 414–469. https://doi.org/10.1016/j.aop.2008.08.008

[5] John F. Donoghue. 1994. General relativity as an effective field theory: The leading quantum corrections. *Physical Review D* 50 (1994), 3874–3888. https://doi.org/10.1103/PhysRevD.50.3874

[6] Astrid Eichhorn and Aaron Held. 2017. Top mass from asymptotic safety. *Physics Letters B* 769 (2017), 29–35. https://doi.org/10.1016/j.physletb.2017.03.024

[7] Bei-Lok Hu and Enric Verdaguer. 2008. Stochastic gravity: Theory and applications. *Living Reviews in Relativity* 11 (2008), 3. https://doi.org/10.12942/lrr-2008-3

[8] Ted Jacobson. 1995. Thermodynamics of spacetime: The Einstein equation of state. *Physical Review Letters* 75 (1995), 1260–1263. https://doi.org/10.1103/PhysRevLett.75.1260

[9] Christian Maes. 2026. What is nonequilibrium? *arXiv preprint arXiv:2601.16716* (2026). arXiv:2601.16716 [cond-mat.stat-mech]

[10] Roser Martin and Enric Verdaguer. 2000. Stochastic semiclassical gravity. *Physical Review D* 61 (2000), 124024. https://doi.org/10.1103/PhysRevD.61.124024

[11] Thanu Padmanabhan. 2010. Thermodynamical aspects of gravity: New insights. *Reports on Progress in Physics* 73 (2010), 046901. https://doi.org/10.1088/0034-4885/73/4/046901

[12] Roberto Percacci. 2017. An Introduction to Covariant Quantum Gravity and Asymptotic Safety. *World Scientific* (2017). https://doi.org/10.1142/10369

[13] Martin Reuter. 1998. Nonperturbative evolution equation for quantum gravity. *Physical Review D* 57 (1998), 971–985. https://doi.org/10.1103/PhysRevD.57.971

[14] Martin Reuter and Frank Saueressig. 2012. Quantum Einstein gravity. *New Journal of Physics* 14 (2012), 055022. https://doi.org/10.1088/1367-2630/14/5/055022

[15] Andrei D. Sakharov. 1968. Vacuum quantum fluctuations in curved space and the theory of gravitation. *Soviet Physics Doklady* 12 (1968), 1040–1041.

[16] Lorenzo Sindoni. 2012. Emergent models for gravity: an overview of free and interacting models. *SIGMA* 8 (2012), 027. https://doi.org/10.3842/SIGMA.2012.027

[17] Erik Verlinde. 2011. On the origin of gravity and the laws of Newton. *Journal of High Energy Physics* 2011 (2011), 29. https://doi.org/10.1007/JHEP04(2011)029

[18] Christof Wetterich. 1993. Exact evolution equation for the effective potential. *Physics Letters B* 301 (1993), 90–94. https://doi.org/10.1016/0370-2693(93)90726-X